Original Research Article

Synthesis of monodisperse magnetic hydroxyapatite/Fe₃O₄ nanospheres for removal of Brilliant Green (BG) and Coomassie Brilliant Blue (CBB) in the single and binary systems.

Zeinab Rezayati zad[1], **Bahareh Mosavi[2]**, **Alireza Taheri** [2*]

[1] Department of Food and Drug, Faculty of Medicine, Ilam University of Medical Sciences, Ilam, Iran
[2] Department of Chemistry, Ilam branch, Islamic Azad University, Ilam, Iran

ARTICLE INFO

ABSTRACT

Conventional wastewater treatments such as chemical coagulation, activated sludge, trickling filter, carbon adsorption and photo-degradation were used for the removal of dyes. The characteristics of (HAp /Fe₃O₄) were investigated using Fourier transform infrared (FTIR) and scanning electron microscope (SEM). The surface area was measured by the Brunauer–Emmett–Teller (BET) nitrogen adsorption apparatus. The crystal phases of the products were characterized by X-ray diffraction with monochromatic Cu Ka radiation. Selectivity analysis for binary system dye removal was investigated. The effect of operational parameter (adsorbent dosage, dye concentration and salt) on dye removal was evaluated in details. UV–vis spectrophotometer was employed for absorbance measurements of samples. The maximum wavelength used for determination of residual concentration of CBB and BG in supernatant solution using UV–vis spectrophotometer were 627 nm, 629 nm, respectively. The effect of adsorbent dosage on dye removal from single (sin.) and binary (bin.) systems was investigated by contacting 10 mL of dye solution with initial dye concentration of 5 mg/L at single (sin.) and binary (bin.). In this paper, monodisperse magnetic HAp (HAp/Fe3O4) microspheres was synthesized and used for the remove dye from single (sin.) and binary (bin.) systems.

GRAPHICAL ABSTRACT
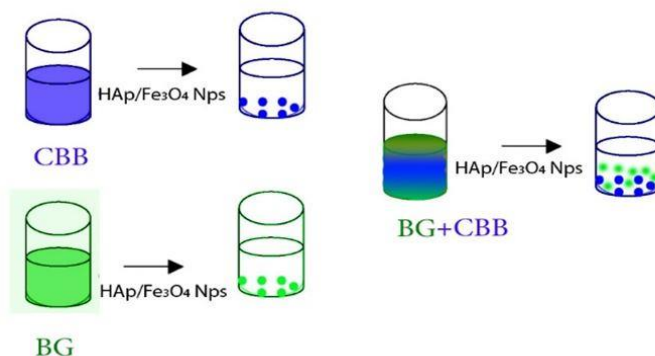
Introduction

Effluents from various industries contain harmful coloring agents, which have to be removed to maintain the quality of the environment. Paper, fabric, leather and dyestuff production are some of the industries that release harmful effluents. Dyes used in various industries have harmful effects on living organisms within short exposure periods [1-3]. The disposal of dyes in wastewater is an environmental problem that causes ill effects to the ecosystem [4-6]. Conventional wastewater treatments such as chemical coagulation, activated sludge, trickling filter, carbon adsorption and photo-degradation were used for the removal of dyes. Brilliant Green (BG) dye is one of the commonly known cationic dyes used for various purposes, e.g. biological stain, dermatological agent, veterinary medicine, an additive to poultry feed to inhibit propagation of mold, intestinal parasites and fungus . It is also used in textile dying and paper printing. Its effluents are generated from rubber and plastic industries [7-12] . This dye is hazardous in case of skin contact, eye contact and ingestion. It is toxic to the lungs, through inhalation. During its decomposition, it may generate carbon dioxide, sulfur oxides and nitrogen oxides. Therefore, it is important to remove brilliant green dye from aqueous solution [9, 13-15]. Coomassie Brilliant Blue (CBB) is a zwitterionic molecule often used to dye proteins in gel electrophoresis that can also be used to visualize penetrance of liquids into hydrogels. An equilibrium measure of this penetrance is known as the partition coefficient. This phenomenon is observed when solutes in a solution diffuse into a hydrogel despite concentration gradients, resulting in a higher concentration of the solute within the hydrogel than within the solution [16-19]. Hydroxyapatite $(Ca_{10}(PO_4)_6(OH)_2$, HAp),one of the most importantinorganic biomaterials has extensive applications in drugdelivery systems[20, 21], photocatalysts[22, 23], and adsorbents because of their high specific surface area, biological,and excellent mechanical properties. In the application of watertreatment, HAp is an ideal material for disposal of long-term contaminanton account of its high sorption capacity for heavy metal and dyes, low water solubility, availability, low cost, and high stability under oxidizing and reducing conditions. However, HAp adsorbents have the common defect of separation difficulty. Therefore, it is essential to develop a sorbent, which can be effectively separated without producing other contaminants after wastewater treatment. It is worth noting that adsorption procedure combined with magnetic separation has found applications in water treatment and environmental cleanup [24-26]. In this paper, monodisperse magnetic HAp (HAp/Fe_3O_4) microspheres was synthesized and used for the remove dye from single (sin.) and binary (bin.) systems (Fig. 1). The characteristics of (HAp /Fe_3O_4) were investigated using Fourier transform infrared (FTIR) and scanning electron microscope (SEM). The surface area was measured by the Brunauer–Emmett–Teller (BET) nitrogen adsorption apparatus. The crystal phases of the products were characterized by X-ray diffraction with monochromatic Cu K_a radiation.
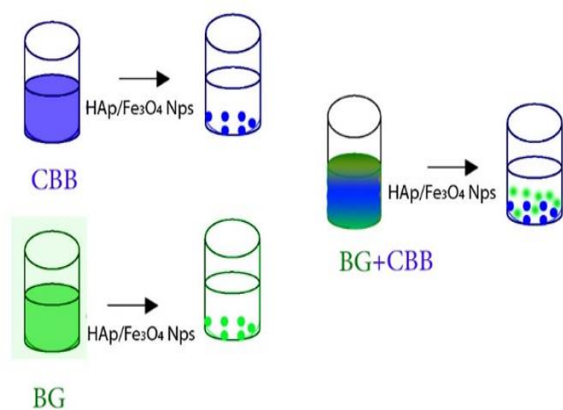
Fig. 1. Dye removal from single and binary systems using (HAp/Fe₃O₄)

Selectivity analysis for binary system dye removal was investigated. The effect of operational parameter (adsorbent dosage, dye concentration and salt) on dye removal was evaluated in details. Sorption isotherms and kinetic models were applied for experimental data analysis [27-30].

2. Materials and method

2.1. Materials

Ferric chloride hexahydrate ($FeCl_3$ $6H_2O$), iron (II) chloride tetrahydrate ($FeCl_2$ $4H_2O$), ammonium hydroxide ($NH_3, H2O$, 28%), calcium chloride anhydrous ($CaCl_2$), sodium carbonate anhydrous (Na_2CO_3), sodium dodecyl sulfate (SDS), sodium phosphate tribasic (Na_3PO_4), Coomassie Brilliant Blue (CBB) and brilliant green(BG), All the chemical regents were used without further purification.

2.2. Sorbents synthesis

2.2.1. Magnetic Fe₃O₄ particles synthesis

In this work, magnetic Fe_3O_4 particles were synthesized by the method by Massart. A combination of $FeCl_3 6H_2O$ (1.7 g) and $FeCl_2 4H_2O$ (0.6 g) were dissolved in 400 mL distilled water under vigorous stirring for 30 min with the protection of nitrogen to obtain a homogeneous yellow solution. Fe_3O_4 particles formed after NH_3, H_2O (3 mL) was dropped into the solution slowly. The obtained products were separated by a magnet and washed several times with distilled water and ethanol, and dried in a vacuum oven at 60 ^0C for 6 h.

2.2.2. Monodisperse magnetic HAp/Fe₃O₄ microspheres synthesis

Monodisperse magnetic HAp/Fe₃O₄ microspheres were synthesized by using $CaCO_3/Fe_3O_4$ microspheres as the sacrificial hard-templates [31-33]. In a typical process, $CaCl_2$ (1.78 g) and SDS (2.3 g) were fully dispersed in 240 mL distilled water under vigorous stirring. The obtained Fe_3O_4 (0.92 g) were added into the solution and vigorously stirred for 15 min.
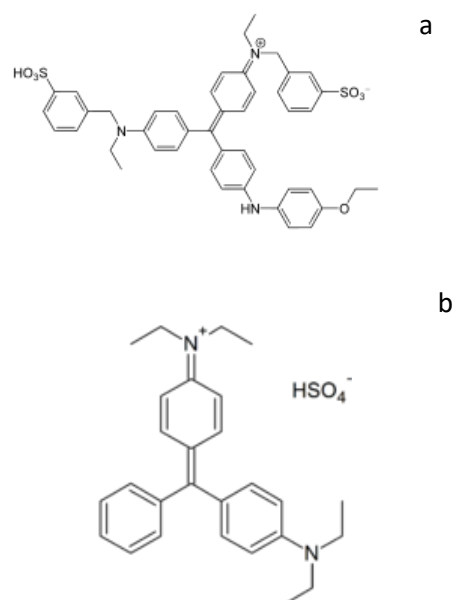
Fig. 2. The chemical structure of dyes (a) CBB, (b) BG.

80 mL aqueous solution containing Na_2CO_3 (1.7 g) was then injected quickly into the above mixed solution to obtain the precipitates with stirring at 25 °C for 1 h. The obtained precipitates ($CaCO_3/Fe_3O_4$) were washed repeatedly with distilled water. The resulting powder (1.5 g) was mixed with 140 mL aqueous solution containing Na_3PO_4 (4.9 g). The suspension was transferred into a Teflon-lined stainless-steel autoclave of 200 mL capacity. The autoclave was maintained at 180 °C for 4 h, followed by cooling to room temperature naturally. The obtained HAp/Fe_3O_4 microspheres were collected using a magnet and washed with distilled water and ethanol, and dried in a vacuum oven at70 °C for 6 h.

2.3. Characterization methods

The functional group of the material was studied using Fourier transform infrared (FTIR) spectroscopy (Perkin-Elmer Spectrophotometer Spectrum One) in the range 3500–500 cm-1. Microstructures of the synthesized products were observed using a field emission scanning electron microscope (SEM, Model S-4800 5.0kv, Hitachi Limited, Japan). The surface area was measured by the Brunauer–Emmett–Teller (BET) nitrogen adsorption apparatus with apparatus PHS-1020(PHSCHINA). The HAp/Fe3O4 microspheres after sorption were separated from aqueous solutions using a magnet, and analyzed via an X-ray photoelectron spectroscopy (XPS, Kratos Axis Ultra DLD, UK) with a monochromic Al Ka X-ray Source (hm = 1486.6 eV).

## 2.4. Adsorption procedure

The dye adsorption measurements were conducted by mixing of monodisperse magnetic HAp (HAp/Fe_3O_4) microspheres containing 10 mL of a dye solution (5 mg/L) at pH = 5.5 The change on the absorbance of all solution samples was monitored and determined at certain time intervals during the adsorption process. At the end of the adsorption experiments, the adsorbent particles were separated by magnetic force and dye concentration was determined. The results

were verified with the adsorption kinetics and isotherm. UV–vis spectrophotometer (Perkin-Elmer Lambda 25 spectrophotometer) was employed for absorbance measurements of samples. The maximum wavelength used for determination of residual concentration of CBB and BG in supernatant solution using UV–vis spectrophotometer were 627 nm, 629 nm, respectively[34, 35]. The effect of adsorbent dosage on dye removal from single (sin.) and binary (bin.) systems was investigated by contacting 10 mL of dye solution with initial dye concentration of 5 mg/L at single (sin.) and binary (bin.) systems was investigated by contacting 10 mL of dye solution with at (HAp/Fe_3O_4) room temperature (25 ° C) for 60 min. The effect of salt (0.1 gr) on dye removal from single (sin.) and binary (bin.) systems was investigated by contacting 10 mL of dye solution (5 mg/L) with(HAp/Fe_3O_4) at room temperature (25 °C) for 60 min. Different salts (kcl, NaCl) were used. The sorption capacity of HAp/Fe_3O_4 was calculated as follows:

$$qe = \frac{C_0 - C_e}{M}V$$

Where qe is the amount of CBB and BG uptake onto per unit weight of the sorbent (mg/g), V is the volume (L) and m is the weight of the sorbent (g).
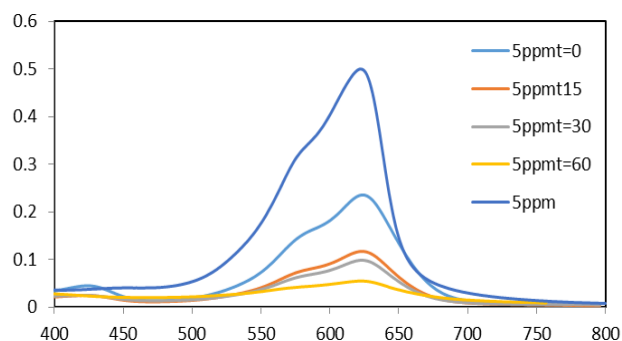
Fig. 3 The maximum wavelength used for determination of residual concentration of CBB and BG.

3. Results and discussion

3.1. Adsorption kinetics study

The adsorption kinetics gives the idea about mechanism of adsorption, from which efficiency of process estimated.

3.1.1. pseudo-first order equation

A linear form of pseudo-first order model is:

$$\log(q_e\text{-}q_t) = \log(q_e)\text{-}(\frac{Kt}{2.303})t$$

where q_e, q_t and k_1 are the adsorbed dye at equilibrium (mg/g), the amount of the adsorbed dye at time t (mg/g) and the equilibrium rate constant of pseudo-first order kinetics (1/min), respectively .

3.1.2. pseudo-second order equation

Linear form of pseudo-second order model was illustrated as[36-40]:

$$\frac{t}{qt} = \frac{1}{k^2 q_e^2} + \left(\frac{1}{q_e}\right)t$$

Where k_2 is the equilibrium rate constant of pseudo-second order (g/mg min)[41-45].

3.1.3. intraparticle diffusion

The possibility of intraparticle diffusion resistance affecting adsorption was explored by using the intraparticle diffusion model as

$$q_t = k_p t + 1 \quad q_t = k_p t + 1$$

Where k_p and I are the intraparticle diffusion rate constant and intercept, respectively. The plot of uptake should be linear when intraparticle diffusion is involved in the adsorption process. In addition, intraparticle diffusion is the rate-controlling step when the lines of uptake pass through the origin then. When the plots do not pass through the origin,

this is indicative of some degree of boundary layer control and it shows that the intraparticle diffusion is not the only rate-limiting step, but also other kinetic models may control the rate of adsorption, all of which may be operating simultaneously [32–34]. To understand the applicability of the pseudo-first order, pseudo-second order and intraparticle diffusion models for the dye adsorption onto HAp/Fe_3O_4 from single (sin.) and binary (bin.) systems at different adsorbent dosage, linear plots of $\log(q_e, q_t)$ versus contact time (t), t/qt versus contact time (t) and q_t against $t^{1/2}$ are plotted. The linearity of the plots (R_2) demonstrates that pseudo-first order and intraparticle diffusion kinetic models do not play a significant role in the uptake of the dye. The linear fit between the t/q_t versus contact time (t) and calculated R_2 for pseudo-second order kinetics model show that the dye removal kinetic can be approximated as pseudo-second order kinetics. In addition, the experimental $q_e((q_e)Exp.)$ values agree with the calculated ones $((q_e)Cal.)$, obtained from the linear plots of pseudo-second order kinetics.

3.2. Adsorption isotherm

The adsorption isotherm studies the relation between the mass of the dye adsorbed onto adsorbent and liquid phase of the dye concentration [45-49]. Several isotherms such as Langmuir, Freundlich and Tempkin models were studied in details. In Langmuir isotherm, a basic assumption is that sorption takes place at specific sites within the adsorbent

Dye removal in binary system follows the Langmuir isotherm. The results show that magnetic nanoparticle has higher dye adsorption capability. Thus, magnetic nanoparticle can be used as an adsorbent [54-58].

3.3. Selectivity analysis for binary system

In this research, selectivity analysis has been also performed for binary system. Usually, the

static distribution coefficient K_D (mL/g) and the separation factor α are utilized to evaluate the molecular selectivity of adsorbent. The higher value of α, the better selectivity is; if α is close to 1.0, the adsorbent has no selectivity. Fig 4 shows the experimental results from the adsorption experiments in binary systems. The results show that α value is close to 1.0. Thus HAP/ Fe_3O_4 has no selectivity [59-64].

3.4. Effect of operational parameter on dye removal

3.4.1. Effect of dye concentration

Adsorption can generally be defined as the accumulation of material at the interface between two phases. The influence of varying the initial dye concentration of dyes on adsorption efficiencies onto HAP/ Fe_3O_4 was assessed. The results are shown in Fig. 4 [65-68]. It is obvious that the higher the initial dye concentration, the high the percentage of dye adsorbed. The amount of the dye adsorbed onto HAP/ Fe_3O_4 decreases with an increase in the initial dye concentration of solution if the amount of adsorbent is kept unchanged.
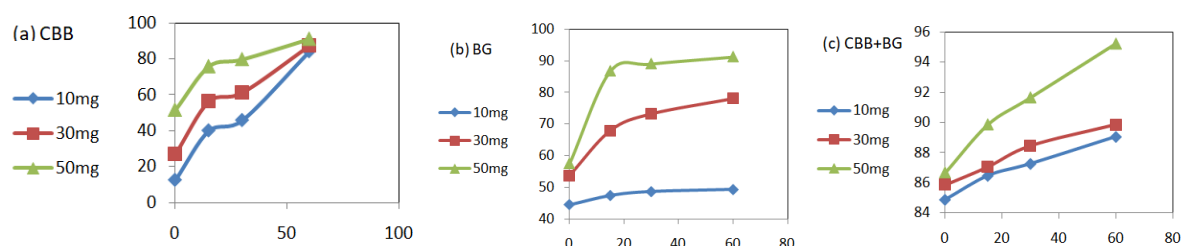
3.4.2. Effect of adsorbent dosage

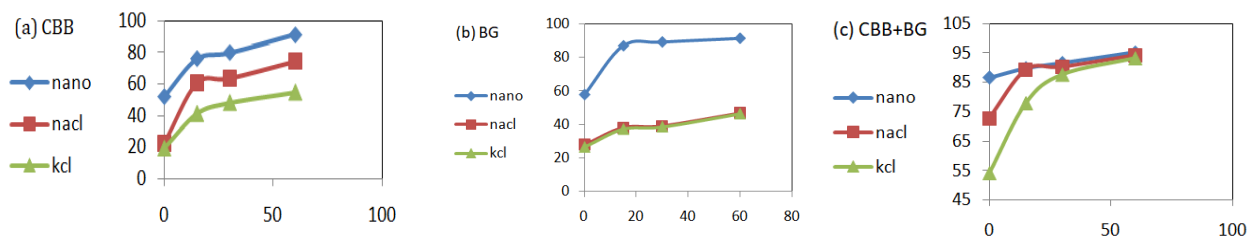The dye removal (%) from single (sin.) and binary (bin.) systems versus time (min) at different HAP/Fe_3O_4 dosages (mg) was shown in Fig. 4. It determines the capacity of the adsorbent for a given initial concentration of dye solution. It was observed that the removal percentage increased rapidly with the increase in the adsorbent dose HAP/ Fe_3O_4, 50 mg and after the critical dose, the removal percentage reached almost a constant value. It can be attributed to overlapping or aggregation of adsorption sites resulting in a decrease in total adsorbent surface area available to the dye and an increase in diffusion path length.

3.4.3. Effect of salt

Inorganic anions of salts may compete for the active sites on the adsorbent surface or deactivate the adsorbent. Thus, dye adsorption efficiency decreases. An important limitation resulting from the high reactivity and non-selectivity of adsorbent is that it also reacts with non-target compounds present in the wastewater such as dye auxiliaries present in the exhausted reactive dye bath. It results higher adsorbent dosage demand to accomplish the desired degree of dye removal efficiency. To investigate inorganic salts effect on dye removal efficiency, KCl, and NaCl were used. Fig. 5 illustrates that dye removal capacity of HAP/Fe_3O_4 from single (sin.) and binary (bin.) systems decreases in the presence of inorganic anions because small anions compete with dyes in adsorption by magnetic nanoparticle.

Fig 4. The effect of adsorbent dosage on dye removal by HAP/Fe_3O_4 from single (sin.) (a) CBB and (b) BG and (c) binary (bin.) systems.

Fig 5. The effect of salt on dye removal by HAP/Fe₃O₄ from single (sin.) and binary (bin.) systems.

3.5. Characterization of HAP/ Fe₃O₄

Characterization of HAP/Fe₃O₄

The FT-IR spectrum was shown in Fig. 6. HAP/Fe₃O₄ has two peaks at 1038 cm⁻¹ and 570 cm⁻¹ that indicate, respectively. SEM are useful for determining the particle shape and appropriate size of the adsorbent. In addition, they are important tools for characterizing the surface morphology and fundamental physical properties of the adsorbent surface. SEM images of Fe_3O_4, $CaCO_3/Fe_3O_4$ and HAP/Fe_3O_4 are shown in Fig. 8. The magnetic Fe_3O_4 nanoparticles had an average diameter of about 500 nm. The hard-template of $CaCO_3/Fe_3O_4$ were comprised of irregular nano-flakes whereas the obtained HAp/Fe_3O_4 microspheres were constructed by uniform nanoparticles. Both $CaCO_3/Fe_3O_4$ and HAp/Fe_3O_4 had a unique size of about 500 nm in diameter. The HAp/Fe_3O_4 had a saturation magnetization of 26.7 emu/g, confirming the Fe_3O_4 nanoparticles dispersed among the HAp crystals. Fig. 8 illustrates the XRD pattern of the Fe_3O_4 and the HAp/Fe_3O_4 [69-71]. It confirmed that the products were composed of a magnetite Fe_3O_4 phase (JCPDS 75-0449) and Hap phase

(JCPDS 86-0740). The nitrogen adsorption desorption isotherm of the HAp/Fe_3O_4 is shown in Fig. 9. According to the BET analysis, the isotherms complied with a combination of type I and type IV, and displayed the H3 hysteresis loop. The plot of the pore size distribution was determined using the Barrett–Joyner–Halenda (BJH) method from the adsorption branch of the isotherm. The average pore size of HAp/Fe_3O_4 microspheres was 11.4 nm and the surface area was 59.4 m2/g, which were beneficial for ion-exchange process [41-43, 72].
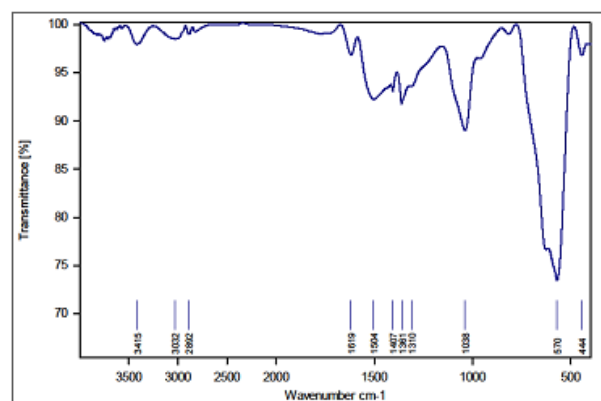
Fig 6. FT-IR spectrum HAP/ Fe₃O₄
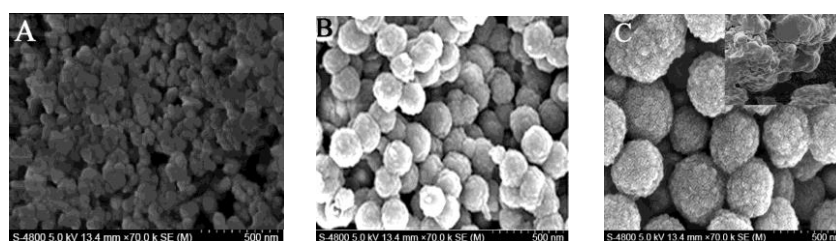
Fig 7. SEM images of (A) Fe3O4, (B) CaCO3/Fe3O4, (c) HAp/Fe₃O₄ microspheres

(a) (b)
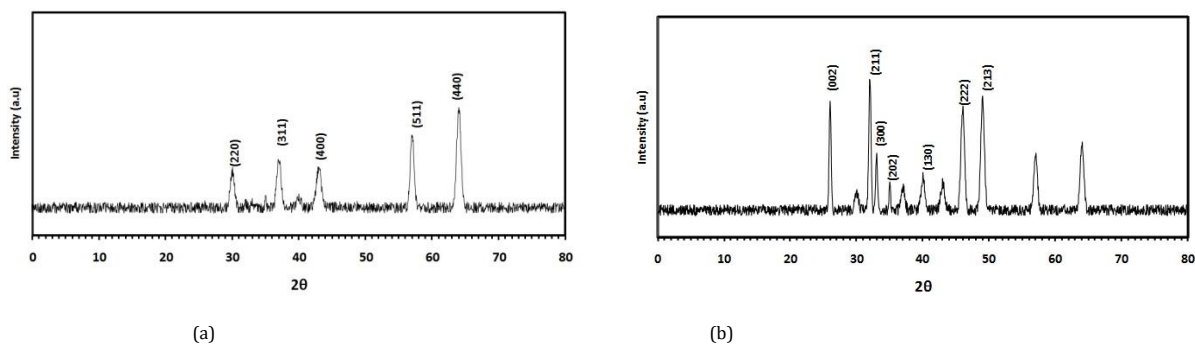
Fig. 8. X-ray diffraction patterns of as-prepared (a). Fe_3O_4 and (b).HAp/Fe_3O_4 microspheres.

Fig. 9. The nitrogen adsorption desorption isotherm of the HAp/Fe3O4

Conclusion

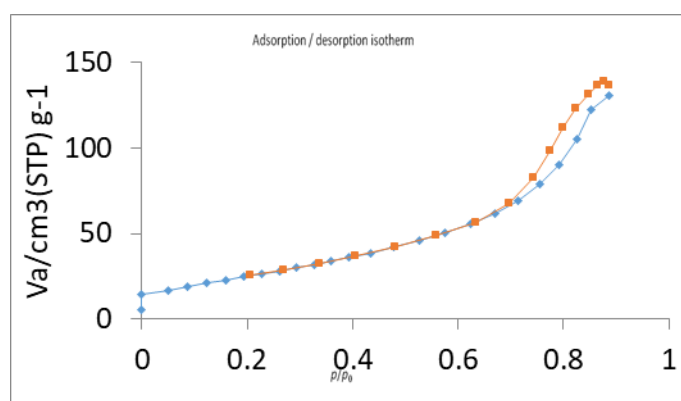Effluents from various industries contain harmful coloring agents, which have to be removed to maintain the quality of the environment. Paper, fabric, leather and dyestuff production are some of the industries that release harmful effluents. Dyes used in various industries have harmful effects on living organisms within short exposure periods The characteristics of (HAp /Fe_3O_4) were investigated using Fourier transform infrared (FTIR) and scanning electron microscope (SEM). The surface area was measured by the Brunauer–Emmett–Teller (BET) nitrogen adsorption apparatus. The crystal phases of the products were characterized by X-ray diffraction with monochromatic Cu Ka radiation. Selectivity analysis for binary system dye removal was investigated. The effect of operational parameter (adsorbent dosage, dye concentration and salt) on dye removal was evaluated in details. UV–vis spectrophotometer was employed for absorbance measurements of samples. The maximum wavelength used for determination of residual concentration of CBB and BG in supernatant solution using UV–vis spectrophotometer were 627 nm, 629 nm, respectively. The effect of adsorbent dosage on dye removal from single (sin.) and binary (bin.)

systems was investigated by contacting 10 mL of dye solution with initial dye concentration of 5 mg/L at single (sin.) and binary (bin.). In this paper, monodisperse magnetic HAp (HAp/Fe$_3$O$_4$) microspheres was synthesized and used for the remove dye from single (sin.) and binary (bin.) systems

References

[1] Z.R. Zad, S.S.H. Davarani, A. Taheri and Y. Bide, A yolk shell Fe3O4@PA-Ni@Pd/Chitosan nanocomposite -modified carbon ionic liquid electrode as a new sensor for the sensitive determination of fluconazole in pharmaceutical preparations and biological fluids. *Journal of Molecular Liquids*, 253 (2018) 233-240.

[2] F. Abdollahi, A. Taheri and M. Shahmari, Application of selective solid-phase extraction using a new core-shell-shell magnetic ion-imprinted polymer for the analysis of ultra-trace mercury in serum of gallstone patients. *Separation Science and Technology*, (2019) 1-14.

[3] R. Jalilian, M. Shahmari, A. Taheri and K. Gholami, Ultrasonic-Assisted Micro Solid Phase Extraction of Arsenic on a New Ion-Imprinted Polymer Synthesized from Chitosan-Stabilized Pickering Emulsion in Water, Rice and Vegetable Samples. *Ultrasonics Sonochemistry*, ????? (2019) 104802.

[4] O.M. Ozkendir, Boron Activity in Metal Containing Materials. *Advanced Journal of Chemistry-Section B*, 2 (2020) 48-54.

[5] Z. Sadiq, G. Yaqub, A. Hamid, H. Sadia and U. Irshad, A Novel Variation in Fischer Indole Reaction for Viable and Rapid Synthesis of 1,2,3,4-Tetrahydro-6,8-Dinitro-9H-Carbazole. *Advanced Journal of Chemistry-Section B*, 2 (2020) 61-63.

[6] A. Usman, V. Fitzsimmons-Thoss and A. Tawfike, Anti-Bacterial, Anti-Oxidant and Cytotoxic Activities of Nimbin Isolated from African Azadirachta Indica Seed Oil. *Advanced Journal of Chemistry-Section B*, 2 (2020) 81-90.

[7] A.S.-M. Ogbuagu and C.I. Okoye, Physico-chemical characterization of Avocado (Persea americana Mill.) Oil from Tree Indonesian Avocado Cultivars. *Progress in Chemical and Biochemical Research*, 3 (2020) 39-45.

[8] T. Panigrahi and A.U. Santhoskumar, Adsorption process for reducing heavy metals in Textile Industrial Effluent with low cost adsorbents. *Progress in Chemical and Biochemical Research*, 3 (2020) 135-139.

[9] A. samimi, S. Zarinabadi, A. Bozorgian, A. Amosoltani, M.S. Tarkesh Esfahani and K. Kavousi, Advances of Membrane Technology in Acid Gas Removal in Industries. *Progress in Chemical and Biochemical Research*, 3 (2020) 46-54.

[10] H. Shamsin Beyranvand, M. Mirzaei Ghaleh Ghobadi and H. Sarlak, Experimental Study of Carbon Dioxide Absorption in Diethyl Ethanolamine (DEEA) in the Presence of Titanium Dioxide (TiO2). *Progress in Chemical and Biochemical Research*, 3 (2020) 55-63.

[11] N. Surma, G. Ijuo and B. Ogoh-Orch, Fuel Gases From Waste High Density Polyethylene (Hdpe) Via Low Temperature Catalytic Pyrolysis. *Progress in Chemical and Biochemical Research*, 3 (2020) 20-30.

[12] M. Tauqir Alam, Abida and M. Asif, A review on analgesic and anti-inflammatory activities of various piperazinyl containing pyridazine derivatives. *Progress in Chemical and Biochemical Research*, 3 (2020) 81-92.

[13] A. samimi, Risk Management in Information Technology. *Progress in Chemical and Biochemical Research*, 3 (2020) 130-134.

[14] A. samimi, Risk Management in Oil and Gas Refineries. *Progress in Chemical and Biochemical Research*, 3 (2020) 140-146.

[15] A. samimi, K. Kavousi, S. Zarinabadi and A. Bozorgian, Optimization of the Gasoline Production Plant in order to Increase Feed.

Progress in Chemical and Biochemical Research, 3 (2020) 7-19.

[16] A. Bozorgian, Z. Arab Aboosadi, A. Mohammadi, B. Honarvar and A. Azimi, Prediction of Gas Hydrate Formation in Industries*. Progress in Chemical and Biochemical Research*, 3 (2020) 31-38.

[17] A. El-Khateeb, Practical Approach for The Identification of Functional Groups in Organic Compounds*. Progress in Chemical and Biochemical Research*, 3 (2020) 147-168.

[18] O. El-Shahaby, F. Reicha, M.M.N. Aboushadi and M. El-Zayat, Green Synthesis and Biological Assessments of Silver Nanoparticles Using the Plant Extract of Crataegus sinaica Boiss. Fruits*. Progress in Chemical and Biochemical Research*, 3 (2020) 105-113.

[19] C. Elliott and A. Vaillant, Antimicrobials and Enterobacterial Repetitive Intergenic Consensus (ERIC) Polymerase Chain Reaction (PCR) Patterns of Nosocomial Serratia Marcescens Isolates: A One Year Prospective Study (June 2013-May 2014) in a Rural Hospital in the Republic of Trinidad and Tobago*. Progress in Chemical and Biochemical Research*, 3 (2020) 105-120.

[20] M. Nabati, E. Pournamdari, V. Bodaghi-Namileh, Y. Dashti-Rahmatabadi and S. Sarshar, Substitution of Carbonyl Group of Ellagic Acid with Silanediol Group for Better Inhibition of VEGFR-2 Kinase Enzyme*. Advanced Journal of Chemistry-Section B*, 2 (2020) 64-72.

[21] M. Nabati, E. Pournamdari, Y. Dashti-Rahmatabadi and S. Sarshar, Withaferin A (WIT) Interaction with beta–Tubulin to Promote Tubulin Degradation: In Silico Study*. Advanced Journal of Chemistry-Section B*, 2 (2020) 26-32.

[22] M. Mirzaei, Drug Discovery: A Non-Expiring Process*. Advanced Journal of Chemistry-Section B*, 2 (2020) 46-47.

[23] M. Molaeian, A. Davood and M. Mirzaei, Non-Covalent Interactions of N-(4-CarboxyPhenyl)Phthalimide with CNTs*. Advanced Journal of Chemistry-Section B*, 2 (2020) 39-45.

[24] K. Harismah and M. Mirzaei, Favipiravir: Structural Analysis and Activity against COVID-19*. Advanced Journal of Chemistry-Section B*, 2 (2020) 55-60.

[25] D.R. Joshi and N. Adhikari, Aflavinines: History, Biology and Total Synthesis*. Advanced Journal of Chemistry-Section B*, 2 (2020) 3-9.

[26] M. Mirzaei, Lab-in-Silico Insights*. Advanced Journal of Chemistry-Section B*, 2 (2020) 1-2.

[27] S.S.H. Davarani, Z. Rezayati-zad, A. Taheri and N. Rahmatian, Highly selective solid phase extraction and preconcentration of Azathioprine with nano-sized imprinted polymer based on multivariate optimization and its trace determination in biological and pharmaceutical samples*. Mater Sci Eng C Mater Biol Appl*, 71 (2017) 572-583.

[28] R. Jalilian and A. Taheri, Synthesis and application of a novel core-shell-shell magnetic ion imprinted polymer as a selective adsorbent of trace amounts of silver ions*. e-Polymers*, 18 (2018) 123-134.

[29] K. Kamari and A. Taheri, Preparation and evaluation of magnetic core–shell mesoporous molecularly imprinted polymers for selective adsorption of amitriptyline in biological samples*. Journal of the Taiwan Institute of Chemical Engineers*, 86 (2018) 230-239.

[30] S. Mohammadi, A. Taheri and Z. Rezayati-zad, Ultrasensitive and selective non-enzymatic glucose detection based on pt electrode modified by carbon nanotubes@ graphene oxide/ nickel hydroxide-Nafion hybrid composite in alkaline media*. Progress in Chemical and Biochemical Research*, 01 (2018) 1-10.

[31] A. babaei, A. Taheri and I. Khani-Farahani, Nanomolar simultaneous determination of levodopa and melatonin at a new cobalt hydroxide nanoparticles and multi-walled

carbon nanotubes composite modified carbon ionic liquid electrode. *Sens. Actuators B,,* 183 (2013) 265– 272.

[32] A. Taheri, R. faramarzi and M. Roushani, Determination of Paraquat in Fruits and Natural Water using Ni(OH)2 Nanoparticles-Carbon Nanotubes Composite Modified Carbon Ionic liquid Electrode. *Anal. Bioanal. Electrochem.*, 7 (2015) 666-683.

[33] Z. Rezayati-zad, S.S.H. Davarani, A. Taheri and Y. Bide, Highly selective determination of amitriptyline using Nafion-AuNPs@branched polyethyleneimine-derived carbon hollow spheres in pharmaceutical drugs and biological fluids. *Biosens Bioelectron*, 86 (2016) 616-22.

[34] A. babaei and A. Taheri, Direct Electrochemistry and Electrocatalysis of Myoglobin Immobilized on a Novel Chitosan-Nickel Hydroxide Nanoparticles-Carbon Nanotubes Biocomposite Modified Glassy Carbon Electrode. *Anal. Bioanal. Electrochem.*, 4 (2012) 342 - 356.

[35] m. Afrasiabi, Z. Rezayati-zad, s. Kianipour, A. babaei and A. Taheri, A Sensor for Determination of Tramadol in Pharmaceutical Preparations and Biological Fluids Based on Multi-Walled Carbon Nanotubes-Modified Glassy Carbon Electrode. *J.Chem.Soc.pak.*, 35 (2013) 1106-1112.

[36] K. Asemave, D.O. Abakpa and T.T. Ligom, Extraction and Antibacterial Studies of Oil from three Mango Kernel obtained from Makurdi - Nigeria. *Progress in Chemical and Biochemical Research*, 3 (2020) 74-80.

[37] N. Bader, A. Elmajbry, Z. Al borki, A. Ahmida and A. Geath, Physico-chemical studies of the complexes of Hippuric acid with Cu(II), Ni(II), Zn(II), and Pb(II) ions in ethanol-water mixed solvent system. *Progress in Chemical and Biochemical Research*, 3 (2020) 1-6.

[38] L. Birichevskaya, M. Vinter, N. Litvinko and A. Zinchenko, Synthesis of liponucleotides using bacterial phospholipase D. *Progress in*

Chemical and Biochemical Research, 3 (2020) 64-73.

[39] M. Bollido and M.A. Cayabo, Beliefs and Practices on Sexuality and Reproductive Health Among Students in Samar College. *Progress in Chemical and Biochemical Research*, 3 (2020) 120-129.

[40] A. Bozorgian, Analysis and simulating recuperator impact on the thermodynamic performance of the combined water-ammonia cycle. *Progress in Chemical and Biochemical Research*, 3 (2020) 169-179.

[41] H. Thacker, V. Ram and P.N. Dave, Plant mediated synthesis of Iron nanoparticles and their Applications: A Review. *Prog. Chem. Biochem. Res.*, 2 (2019) 84-91.

[42] O.E. Thomas, O.A. Adegoke, A.F. Kazeem and I.C. Ezeuchenne, Preferential Solvation of Mordant Black and Solochrome Dark Blue in Mixed Solvent Systems. *Prog. Chem. Biochem. Res.*, 2 (2019) 40-52.

[43] C.A. Ukwubile, E.O. Ikpefan, M.S. Bingari and L. Tam, Acute and subchronic toxicity profiles of Melastomastrum capitatum (Vahl) Fern. (Melastomataceae) root aqueous extract in Swiss albino mice. *Prog. Chem. Biochem. Res.*, 2 (2019) 74-83.

[44] A.S. Zaek, B.A. Benhamed, M.A. Al shahomy, R. kamour and A. Eshames, Comparative study of pharmaceutical content of three different cardio vascular system drugs marketed in Tripoli- Libya. *Prog. Chem. Biochem. Res.*, 2 (2019) 6-12.

[45] Abida, M. Tauquir Alam and M. Asif, Study of Some Hyndantion Derivatives as Anticonvulsant Agents. *Progress in Chemical and Biochemical Research*, 3 (2020) 93-104.

[46] A. Alkherraz, O. Hashad and K. Elsherif, Heavy Metals Contents in Some Commercially available Coffee, Tea, and Cocoa Samples in Misurata City – Libya. *Prog. Chem. Biochem. Res.*, 2 (2019) 99-107.

[47] K.K. Alisher, T.S. Khamza and Y.S. Ikbol, Quantum-chemical study of geometric and

energy characteristics of some bases of shiff gossipol. *Prog. Chem. Biochem. Res.*, 2 (2019) 1-5.

[48] M. Aghazadeh, Tertiary cyclic amides in Vilsmeier type reaction with indoles. *Prog. Chem. Biochem. Res.*, 2 (2019) 34-39.

[49] M.K. Aadesariya, V.R. Ram and P.N. Dave, Investigation of phytochemicals in methanolic leaves extracts of Abutilon pannosum and Grewia tenax by Q-TOF LC/MS. *Prog. Chem. Biochem. Res.*, 2 (2019) 13-19.

[50] M. Davarpanah, H. Abbasi, M. Nabati, H. Sabahnoo, V. Bodaghi-Namileh, M. Mazidi, H. Movahhed-Tazehkand and H. Mohammadnejad-Mehrabani, Kit formulation of active pharmaceutical ingredient d,l-HMPAO as a brain perfusion diagnostic system. *Progress in Chemical and Biochemical Research*, 2 (2019) 185-191.

[51] M. Asif and I. Mohd, Synthetic methods and pharmacological potential of some cinnamic acid analogues particularly against convulsions. *Progress in Chemical and Biochemical Research*, 2 (2019) 192-210.

[52] M. Asif and I. Mohd, Prospects of Medicinal Plants Derived Nutraceuticals: A Re-emerging New Era of Medicine and Health Aid. *Progress in Chemical and Biochemical Research*, 2 (2019) 150-169.

[53] K. Asemave and T. Anure, The bioactivities of the neem (seeds and leaves) against Callosobruchus maculatus on a Vigna Subterranean L. *Prog. Chem. Biochem. Res.*, 2 (2019) 92-98.

[54] W.H. Elobeid and A.A. Elbashir, Development of chemically modified pencil graphite electrode based on benzo-18-crown-6 and multi-walled CNTs for determination of lead in water samples. *Prog. Chem. Biochem. Res.*, 2 (2019) 24-33.

[55] M. Eldefrawy, E.G.A. Gomaa, S. Salem and F. Abdel Razik, Cyclic Voltammetric studies of calcium acetate salt with Methylene blue (MB)

Using Gold Electrode. *Prog. Chem. Biochem. Res.*, 1 (2018) 11-18.

[56] O.A. El-Shahaby, M. El-Zayat, G. Abd El-Fattah and M.M. El-Hefny, Evaluation of the biological activity of Capparis spinosa var. aegyptiaca essential oils and fatty constituents as Anticipated Antioxidant and Antimicrobial Agents. *Progress in Chemical and Biochemical Research*, 2 (2019) 211-221.

[57] O. El-Shahaby, M. El-Zayat, R. Rabei and H.S. Aldesuquy, Phytochemical constituents, antioxidant activity and antimicrobial potential of Pulicaria incisa (lam.) DC as a folk medicinal plant. *Progress in Chemical and Biochemical Research*, 2 (2019) 222-227.

[58] A. El-Khateeb, M.H. Mahmoud and M. Fakih, Comparative study on different horizontal subsurface substrates in flow wetlands. *Prog. Chem. Biochem. Res.*, 2 (2019) 20-23.

[59] A. John and R.A. Oluwafemi, Hematology and Serum Biochemical Indices of Growing Rabbits Fed Diet Supplemented with Different Level of Indigofera Zollingeriana Leaf Meal. *Progress in Chemical and Biochemical Research*, 2 (2019) 170-177.

[60] A.U. Itodo, O.M. Itodo, E. Iornumbe and M.O. Fayomi, Sorptive chelation of metals by inorganic functionalized organic WOx–EDA nanowires: adsorbent characterization and isotherm studies. *Prog. Chem. Biochem. Res.*, 1 (2019) 50-59.

[61] A. Hayat, T.M. Jahangir, M. Yar Khuhawar, M. Alamgir, R. Ali, A. Ali and S.G. Musharraf, Determination of Important Phenolic Compounds in Pakistani Brown Rice Varieties in Controlled, Germinated and Fermented Conditions by High Performance Liquid Chromatography. *Prog. Chem. Biochem. Res.*, 2 (2019) 134-142.

[62] E.G.A. Gomaa, M.A. Berghout, M.R. Moustafa, F.M. El Taweel and H.M. Farid, Thermodynamic and Theoretical solvation parameters for 2-amino-4,5-dimethylthiophene-3-carboxamide(ADTC) in

Ethanol and Mixed EtOH-H2O solvents*. Prog. Chem. Biochem. Res.*, 1 (2018) 19-28.

[63] V. Foram, K. Pooja, V. R. Ram and P.N. Dave, Sex Determination in Papaya: A mini review*. Progress in Chemical and Biochemical Research*, 2 (2019) 228-234.

[64] A. Foda, H. Mosallam, A. El-Khateeb and M. Fakih, Cinnamomum zeylanicum Extract as Green Corrosion Inhibitor for Carbon Steel in Hydrochloric Acid Solutions*. Prog. Chem. Biochem. Res.*, 2 (2019) 120-133.

[65] A.R. Moosavi-Zare, H. Goudarziafshar and Z. Jalilian, Tandem Knoevenagel-Michael-cyclocondensation reaction of malononitrile, various aldehydes and barbituric acid derivatives using isonicotinic acid as an efficient catalyst*. Prog. Chem. Biochem. Res.*, 2 (2019) 59-63.

[66] S. Mohammadi, A. Taheri and Z. Rezayati-Zad, Ultrasensitive and selective non-enzymatic glucose detection based on pt electrode modified by carbon nanotubes@ graphene oxide/ nickel hydroxide-Nafion hybrid composite in alkaline media*. Prog. Chem. Biochem. Res.*, 1 (2018) 1-10.

[67] E. Khan Muluh, A. Odokpe Ugbede and T.A. Tor-Anyin, screening of cassia sieberiana (fabaceae) leaf extract for in-vitro anti microbial and anti-ulcer activities*. Prog. Chem. Biochem. Res.*, 2 (2019) 143-149.

[68] M.E. Khan, A.S. Adeiza, T.A. Tor-Anyiin and A. Alexander, Isolation and characterization of spinasterol from crossopterxy febrifuga stem bark*. Prog. Chem. Biochem. Res.*, 2 (2019) 68-73.

[69] O. Solomon, W. Rabiu Saidu Umar, H. Sanusi Wara, A. Sadiq Yakubu, M. Michael Azubuike, M. Asugu Mary and H. Louis, Antiulcerogenic Activity of methanol extract and solvent fractions of Stem Bark of Lannea acida (A. Rich) Against Ethanol-Induced Gastric Mucosal Injury in Albino Rats*. Prog. Chem. Biochem. Res.*, 1 (2018) 29-39.

[70] M. Nabati, V. Bodaghi-Namileh and S. Sarshar, Molecular Modeling of the antagonist compound esketamine and its molecular docking study with non-competitive N-methyl-D-aspartate (NMDA) receptors NR1, NR2A, NR2B and NR2D*. Prog. Chem. Biochem. Res.*, 2 (2019) 108-119.

[71] S.M. Motevalli and F. Mirzajani, Biotic / Abiotic Stress Influences on Human Epidermal Keratinocyte Cells*. Prog. Chem. Biochem. Res.*, 2 (2019) 53-58.

[72] A. Sysa, M. Labai, E. Kvasyuk, U. Ivuts and M. Khanchevskii, Influence of arabinofuranosylcytosine-5`-monophosphate and its emoxipin salt on viability and functional status of peripheral blood lymphocytes subpopulations*. Progress in Chemical and Biochemical Research*, 2 (2019) 178-184.